ELSEVIER

Polymer 42 (2001) 991–1000

polymer

www.elsevier.nl/locate/polymer

The crystallisation of blends of syndiotactic polystyrene and polyphenylene ether

S. Duff[a], S. Tsuyama[b], T. Iwamoto[b], F. Fujibayashi[b], C. Birkinshaw[a,*]

[a]*Department of Material Science and Technology, University of Limerick, Limerick, Ireland*
[b]*Asahi Chemical Co. Ltd, Polymer Development Laboratory, Kurashiki, Japan*

Received 15 December 1999; received in revised form 9 May 2000; accepted 9 June 2000

Abstract

Blends of syndiotactic polystyrene (SPS) with polyphenylene ether (PPE) have been prepared to determine the effect of blending on the crystallisation mechanism of SPS. The miscibility of the blend was confirmed by both differential scanning calorimetry and dynamic mechanical thermal analysis. Crystallisation of the blends was studied under isothermal and non-isothermal conditions using differential scanning calorimetry, and the isothermal crystallisation kinetics were interpreted using the Avrami equation with the Avrami exponent, *n*, determined as a non-integer value varying between 2 and 3. The nucleation mode was determined as existing within regime II crystallisation, as defined by Lauritzen–Hoffman theory. Non-isothermal crystallisation kinetics were estimated using Nakamura's model. X-ray diffraction was used to determine that the SPS polymorph present was the β-form. The diffuse scattering was shown to increase with PPE content, particularly with blends prepared using higher molecular weight PPE. Overall, the results indicate that the crystallisation of SPS is affected by blending with PPE, with the melting enthalpy of SPS decreasing and the half-time to crystallisation increasing with PPE concentration. This is thought to occur because of the lack of flexibility in the PPE chain compared with the SPS chain. © 2000 Elsevier Science Ltd. All rights reserved.

Keywords: Syndiotactic polystyrene; Polyphenylene ether; Blends

1. Introduction

Syndiotactic polystyrene (SPS) can be synthesised with a degree of stereospecificity of up to 96%, and compared to its isotactic counterpart it can crystallise at a high rate to give a final crystal content of about 60% [1]. The polymer has the relatively high melting point of 270°C [2] and has good chemical resistance, comparable with other olefin polymers [3]. The commercial viability of SPS will depend on control of crystallisation under various processing conditions and so information on the crystallisation mechanism is of value.

The crystallisation kinetics of SPS have been studied under isothermal and non-isothermal conditions using predominantly scanning calorimetry and optical microscopy [4–6]. For SPS crystallised from the melt, it was found that crystallites had a spherulitic morphology and both the spherulite growth rate and overall crystallisation rate were dependent on crystallisation temperature and sample preparation method [4]. Segregation of impurities and non-crystallisable molecules was observed during the crystallisation process and the influence of tacticity was confirmed, with SPS crystallising more rapidly than isotactic polystyrene for the same value of undercooling. More recent work has concentrated on the use of models to predict crystallisation kinetics and behaviour over a wide temperature range. Wesson [5] used a dynamic model to investigate non-isothermal crystallisation of SPS and concluded that the crystallisation rate is molecular weight dependent. At lower temperatures lower molecular weight material has the fastest crystallisation rate, while at higher temperatures higher molecular weight polymer crystallised the fastest. The crossover is believed to represent a change from diffusion limited to thermodynamically controlled crystallisation. The equilibrium melting temperature T_m^0 was taken to be 278°C. St Lawrence et al. [6] examined the isothermal crystallisation of samples over the temperature range T_g to T_m, (100–270°C) and the experimental measurements at both high and low temperatures of transformation could be closely fitted to the predicted rate constant. It was found that to estimate the crystallisation parameters most accurately, the data had to be fitted simultaneously at high and low temperatures and a relatively high value for the equilibrium melting temperature (288°C) had to be used.

Blends of SPS with other thermoplastics may offer some

---

[*] Corresponding author. Tel.: +353-61-202700; fax: +353-61-330316.

0032-3861/01/$ - see front matter © 2000 Elsevier Science Ltd. All rights reserved.
PII: S0032-3861(00)00440-7

technical advantages and so it is of interest to examine the effects of blending on the crystallisation process. A limited number of investigations have been reported. For example Cimmino et al. [7] examined blends of SPS with polyphenylene ether (PPE) and poly vinyl methyl ether to determine the influence of tacticity and miscibility on the crystallisation behaviour of SPS, and Guerra et al. [8] examined blends of SPS with PPE. The latter investigation concentrated on the effect that the blending conditions had on the SPS morphology.

The objective of the work reported here was to identify the effect that blending SPS with PPE had on the crystallisation behaviour of the SPS. This particular material combination is potentially of use as an engineering thermoplastic and an understanding of the crystallisation processes is important for such an application. The experimental observations have been made using thermal analysis to study crystallisation kinetics, and as the literature reports [8] a number polymorphs for SPS, X-ray diffraction experiments have been used to establish the crystal structure in the materials investigated.

The results obtained from the crystallisation experiments have been analysed using the Avrami and the Lauritzen–Hoffman approaches to define the crystallisation regime present. The Avrami equation [9,10] is

$$\chi = 1 - \exp\{ -k(t - t_i)^n \} \qquad (1)$$

where χ is the degree of crystallinity at time t, k is the kinetic rate constant, t_i is the induction time of nucleation and n is the Avrami exponent. The kinetic parameters are determined in the usual way by taking a plot of $\log(-\ln(1 - \chi))$ versus $\log(t - t_i)$ to yield a straight line of slope n and intercept $\log k$. An Avrami exponent of $n \approx 3$ indicates spherulite structures, assuming instantaneous nucleation, while $n \approx 2$ indicates disc-like growth. A difficulty can arise from choice of t_i values as it may be experimentally difficult to distinguish between a genuine induction time associated with organisation of chain segments into nanodomains, and delays arising from the thermal response of the measuring instrument. The assumed value will affect the results from the Avrami equation.

According to the Lauritzen–Hoffman theory [11] the growth rate of polymer crystals is described by

$$G = G_0 \exp[-U^*/\mathrm{R}(T - T_\infty)] \exp[-A/T(\Delta T)f] \qquad (2)$$

where G_0 is a pre-exponential factor containing quantities not strongly dependent upon temperature, U^* is a universal constant characteristic of the activation energy of chain motion (reptation) in the melt, R is the gas constant, T is the crystallisation temperature, T_∞ is the theoretical temperature at which all motion associated with viscous flow or reptation ceases, A is the nucleation parameter, $\Delta T = T_m^0 - T$ and is the undercooling, and $f = 2T/T_m^0 + T$, a temperature correction factor. It is considered that for the system and cooling conditions under investigation here, crystallisation is likely to occur within regimes I or II, but not within regime III. With regime I crystallisation a single nucleus on the advancing surface of the crystal rapidly grows to form a new layer leading to a growth pattern which is smooth, and in this case,

$$A_{(\mathrm{I})} = 4b\sigma\sigma_e T_m^0/(\Delta H_f)\mathrm{k} \qquad (3)$$

where b is the layer thickness, σ is the lateral surface free energy, σ_e is the fold surface free energy, T_m^0 is the equilibrium melting temperature, ΔH_f is the enthalpy of fusion and k is Boltzmann's constant. For regime II crystallisation, new surface nuclei form before the previous layer is complete, leading to an irregular crystal front, in which case

$$A_{(\mathrm{II})} = 2b\sigma\sigma_e T_m^0/(\Delta H_f)\mathrm{k} \qquad (4)$$

The value of A depends upon the crystallisation regime and as

$$\ln G = \ln G_0 - [U^*/\mathrm{R}(T - T_\infty)] - [A/T(\Delta T)f] \qquad (5)$$

a plot of $[1/T(\Delta T)f]$ against $[\ln G + U^*/\mathrm{R}(T - T_\infty)]$ will have slope of $-A$ and an intercept of $\ln G_0$, allowing identification of changes of regime from changes in slope.

Lauritzen–Hoffman theory was originally derived for use in analysing the crystallisation kinetics of homopolymers. However it has also been applied to polymer–diluent [12–14] and polymer–polymer systems [15,16]. The use of these equations for such systems is acceptable where the blend components are immiscible. In such cases the crystalline component will generally crystallise in isolated domains, exhibiting properties characteristic of the homopolymer [17]. However, if a blend consisting of an amorphous and a crystalline component is miscible, then the behaviour of the amorphous component increases in importance. Specifically, if diffusion of the amorphous polymer is limited in some way, then there is a possibility of a build up of that polymer at the crystalline–amorphous interface leading to a decrease in the spherulite growth rate, and a growth process dominated by displacement phenomena. With this in mind, the Lauritzen–Hoffman equation has been modified to take into account the presence of a second component which effectively acts as a diluent of the system [18]

$$\ln G - \ln \phi + U^*/\mathrm{R}(T - T_\infty) - 0.2T_m^0 \ln \phi/\Delta T = \alpha$$
$$= \ln G_0 - A/T(\Delta T)f \qquad (6)$$

where ϕ is the volume fraction of the crystalline polymer. Thus if α is plotted against $1/T(\Delta T)f$, a straight line is expected with slope A and intercept $\ln G_0$.

Crystal growth from the melt is generally considered to be heterogeneous in nature and it can be proposed that a useful proportionality exists between k (the kinetic constant from Eq. (1)), and G, specifically, that $k \approx G^{n+1}$ (where n is the measured Avrami exponent). The parameters k and G are usually related as $k \approx G^n$ for heterogeneous nucleation, but experience has shown that analysis of the blend crystallisation data on this basis does not lead to linear

Table 1
Summary of blends prepared

Blend series	SPS M_w	PPE M_w	Blend ratios
1	292 000	43 800	100/0, 85/15, 75/25, 65/35, 50/50
2	162 000	43 800	100/0, 75/25, 50/50
3	400 000	43 800	100/0, 75/25, 50/50
4	292 000	36 500	75/25, 50/50
5	292 000	70 000	75/25, 50/50

relationships, whereas using $k \approx G^{n+1}$ does. This may be necessary because of underestimation of the Avrami exponent, perhaps because of the previously mentioned difficulties in determination of crystallisation induction times. The relationship is then used in the following way:

$$k^{1/(n+1)} \approx G \tag{7}$$

which leads to

$$\ln(k^{1/(n+1)}) - \ln \phi + U^*/\mathrm{R}(T - T_\infty) - 0.2T_\mathrm{m}^0 \ln \phi/\Delta T = \ln G_1 - A/T(\Delta T)f \tag{8}$$

The isothermal crystallisation rate data is initially plotted according to the Avrami equation, allowing values of k and n to be determined for various crystallisation temperatures. These are then substituted into Eq. (7). Hoffman found that $U^* = 1500\ \mathrm{cal\ mol^{-1}}$ and $T \approx T_\mathrm{g} - 30\ \mathrm{K}$ by fitting the crystallisation kinetic data for various polymers [12]. T_m^0 is estimated using the Hoffman–Weeks method [19].

It is possible to obtain an indication of whether crystallisation is regime I or regime II using the Lauritzen Z test [12]. The Z test equation is

$$Z = iL^2/4g \tag{9}$$

where Z is a dimensionless quantity and L is the substrate length. Z can be approximated by

$$Z \approx 10^3(L/2a_0)^2 \exp[-X/T\Delta T)] \tag{10}$$

where a_0 is the fold width parallel to the growth face. For regime I, $X = A$, and $Z \leq 0.01$. For regime II, $X = 2A$ and $Z \geq 1$. The value of A is determined from the slope of the Lauritzen–Hoffman plot and substituted into Eq. (10). Thus a range of L values is determined for each regime. It is generally found that one regime will produce acceptable values of L, whereas the other will present unrealistic values.

Non-isothermal crystallisation processes can be modelled using integral or differential expressions of the Avrami equation with a temperature dependent kinetic constant. Nakamura et al. [20] proposed that the relative crystallinity at time t, $\chi(t)$, could be expressed as

$$\chi(t) = 1 - \exp\left[-\int_0^t K(T)\,\mathrm{d}t\right]^n \tag{11}$$

where $K(T) = k(T)^{1/n}$; k is the rate constant of isothermal crystallisation and n is the Avrami exponent. Wesson [5] has used the crystal linear growth rate, G, as an estimate for k. Eq. (11) assumes that the crystal growth rate divided by the probability to form new nuclei is constant and is not a function of temperature. Eq. (11) can be expressed as a function of temperature by incorporating the cooling rate of transformation, $\Phi = \mathrm{d}T/\mathrm{d}t$, leading to

$$\chi(T) = 1 - \exp\left\{-\frac{1}{\Phi}\int_{T(0)}^{T(t)} (G(T)^{1/n})\,\mathrm{d}T\right\}^n \tag{12}$$

This expression is used to model the non-isothermal crystallisation process. Initial values are assumed for the parameters G_0, U, A and n (contained within the expression for G). These values are then altered in a regressional manner until the model fits the non-isothermal crystallisation data. It should be noted that the values obtained for the crystallisation parameters are intended only for use in highlighting overall trends within the blend system. An integration software package such as SIMUSOLV would be required to obtain strictly qualitative data [21].

2. Experimental

The SPS used was synthesised by Asahi Chemical Company using a metallocene catalyst. Materials with weight-average molecular weights of 162 000, 292 000 and 400 000 were used and are designated SPS162, SPS292 and SPS400, respectively. PPE was also synthesised by Asahi Chemicals and had weight average molecular weights of 36 500, 43 800 and 70 000. These materials were designated PPE37, PPE44 and PPE70, respectively.

Blends were prepared by dissolving polymer components to a total weight of 15 g in 485 g of ethylbenzene and heating to 135°C under flowing nitrogen. This mixture was then refluxed for 3 h and then cooled to room temperature. Methanol was added to bring the total volume to approximately 1 l and the resulting polymer suspension stirred for 1 h and then filtered under reduced pressure. The powder precipitate was dried in a vacuum oven at 200°C for 3 h. Pure SPS was also subjected to the same solvent and temperature treatment.

Blends and also pure SPS were melt crystallised by compression moulding. The mould was preheated to 330°C before powder was introduced. Pressing was then carried out at a temperature of 330°C and a pressure of $70\ \mathrm{kg\ cm^{-2}}$ for 2 min. The mould was then allowed to cool slowly to room temperature before removal of the product.

Four different SPS/PPE blend ratios were used, 85/15, 75/25, 65/35 and 50/50. The total series of blends prepared is given in Table 1.

Crystallisation experiments were carried out in a Perkin–Elmer DSC7 calorimeter. Samples were heated to 350°C held at that temperature for 2 min and then cooled to the

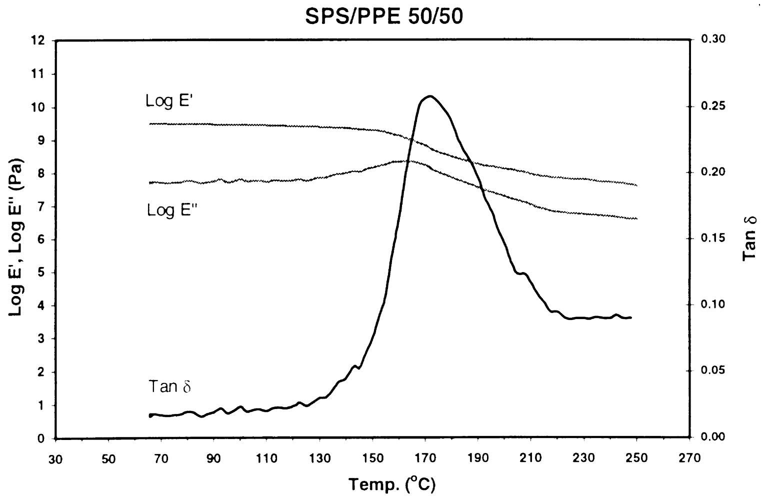

Fig. 1. DMTA response of a SPS292/PPE44 50/50 blend.

crystallisation temperature, T_c held isothermally for a time t and then cooled to 30°C. Sample size was 10 mg and heating and cooling was carried out at 80°C min^{-1}. T_c was initially set at the temperature of the onset of crystallisation in a dynamic DSC experiment and in subsequent experiments 2°C increments in T_c were used.

Melting curves were also obtained using DSC. For most of the work a Perkin–Elmer DSC7 was again used. Samples were initially heated to 350°C to eliminate previous thermal history and then quenched to the selected crystallisation temperature and held isothermal until crystallisation was complete, in 5–30 min, and then melted at 20°C min^{-1}. The melting temperature was taken as the onset of the endothermic peak, as the possible presence of two polymorphs can give a composite melting event. The equilibrium melting temperature was estimated using the Hoffman–Weeks method, whereby T_m^0 is the intercept of the extrapolated T_m values with the line defined by $T_m = T_c$. A limited number of scans were also carried out using a TA Instruments temperature modulated DSC. Samples were first pre-melted in the conventional DSC and the temperature modulated run was carried out at a frequency of 60 s and an amplitude of 0.5°C with a heating and cooling rate of 5°C min^{-1}.

The isothermal data was plotted according to the Avrami equation allowing values of k and n to be determined for the various crystallisation temperatures. These values were then used to create a plot of the general Lauritzen–Hoffman form which in turn allows any changes in the crystallisation regime to be identified.

For the non-isothermal measurements the samples were initially held at 50°C, heated to 350°C, held isothermal for 2 min, cooled to 50°C, held isothermal for 2 min and then reheated to 350°C. The heating and cooling rate used was 20°C min^{-1}.

Wide angle X-ray diffraction patterns were obtained using a Philips powder diffractometer with Cu Kα radiation at an accelerating voltage of 40 kV and a beam current of 35 mA. Dynamic mechanical analysis was carried out on a

Table 2
Variation of glass transition temperature and T_m^0 with blend composition, as determined by calorimetry

SPS292/PPE44	100/0	85/15	75/25	65/35	50/50
T_g (°C)	100.0	111.7	124.3	131.9	139.0
T_m^0 (°C)	273.1	273.0	271.0	268.3	261.4
SPS162/PPE44	100/0	85/15	75/25	65/35	50/50
T_g (°C)	99.4	–	125.1	–	157.0
SPS400/PPE44	100/0	85/15	75/25	65/35	50/50
T_g (°C)	99.9	–	124.0	–	157.0
SPS292/PPE37	100/0	85/15	75/25	65/35	50/50
T_g (°C)	100.0	–	125.5	–	137.9
SPS292/PPE70	100/0	85/15	75/25	65/35	50/50
T_g (°C)	100.0	–	126.4	–	145.1

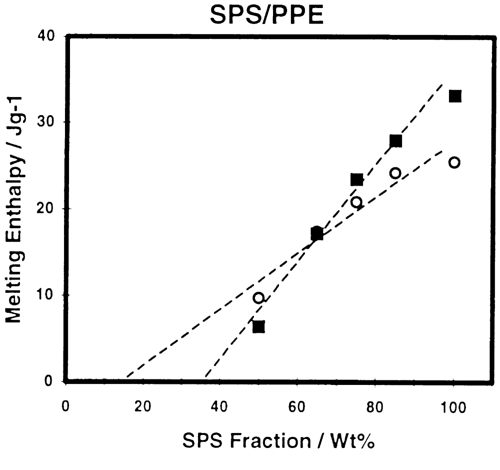

Fig. 2. Melting enthalpy, of blends of SPS292/PPE44 measured using modulated DSC (■) and conventional DSC (○).

Rheometrics DMTA IV instrument at a frequency of 10 Hz and a heating rate of 20°C min^{-1}.

3. Results and discussion

3.1. Crystallisation kinetics

Fig. 1 shows the DMTA response of a SPS292/PPE44, 50/50 blend, and the single glass transition, occurring around 175°C, confirms that the blend components are miscible. Table 2 details the T_g values of blends of the same materials measured by conventional DSC and also the T_m^0 values of these blends. The T_g values recorded do not show a dependence on the molecular weight of the SPS but do show some dependence on PPE molecular weight. Fig. 2 is a plot of melting enthalpy, measured using both modulated DSC and conventional DSC, of the same blends against blend composition. The relative merits of results from the two types of DSC instrument used here have been the subject of much debate, and as this is ongoing both sets of results are offered. In both cases the observations suggest that the crystallisation of SPS is influenced by the presence of the PPE.

Fig. 3(a)–(c) shows the half-time to crystallisation, $t_{1/2}$ for the blends as a function of the crystallisation temperature, blend composition and molecular weight. The half-time is seen to increase with PPE content. SPS molecular weight does not significantly affect $t_{1/2}$ but the PPE molecular weight does have an influence.

Fig. 4 shows a plot of $\log(-\ln(1-\chi)$ versus $\log(t-t_i)$ which gives the Avrami exponent n, as the slope of the line and the rate through the intercept $\log k$. In the case of the blends examined, the exponent obtained has values of between 2 and 3, which suggests the presence of mixed growth and crystallisation mechanisms at each blend ratio. The values of the Avrami exponent do not appear to change with either SPS or PPE molecular weight. It was not possible to determine the exponent at the 50/50 blend ratio with PPE of M_w 70 000 because of the slow rate of crystallisation of that particular blend.

The Lauritzen–Hoffman plots are given in Fig. 5, and the possible values of L were determined as ≤0.5–5.0 Å for regime I, and ≥20–800 Å for regime II. As the latter range is more realistic, crystallisation is taken to occur in regime II. Fig. 6 shows a typical relative crystallinity against temperature plot for non-isothermal conditions, with the

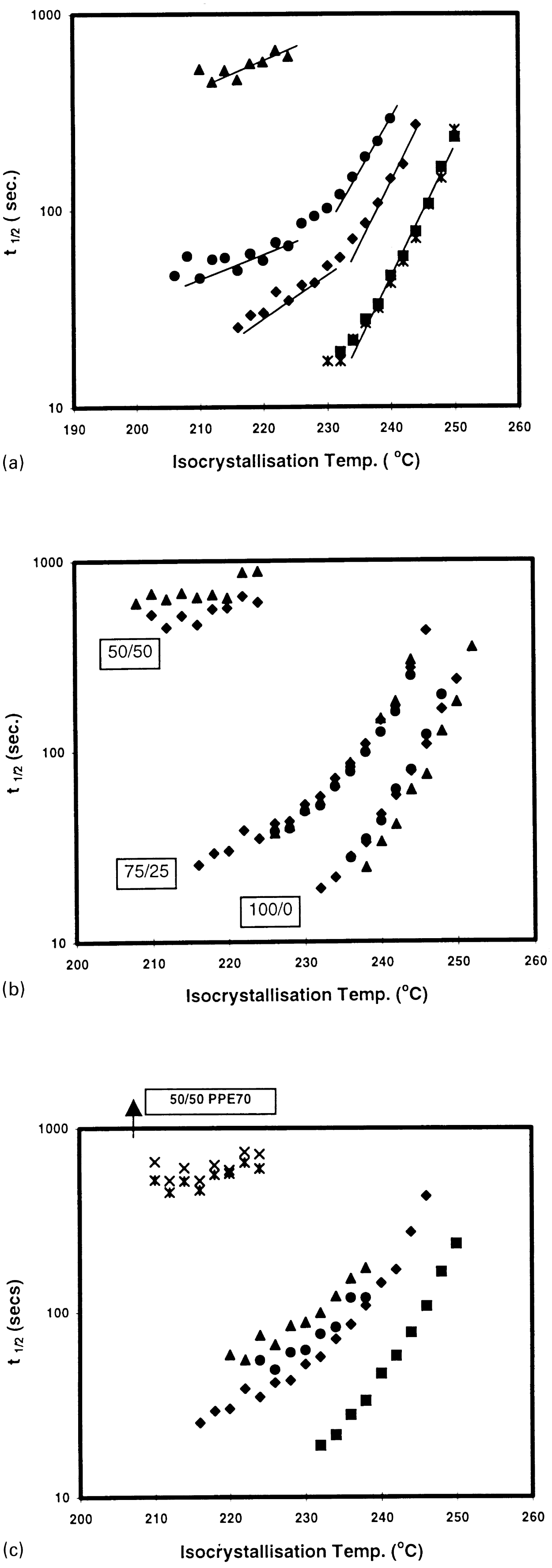

Fig. 3. (a) Half-time to crystallisation, $t_{1/2}$ for blends of SPS292/PPE44 as a function of the crystallisation temperature, pure SPS (■), SPS/PPE 85/15 (★), 75/25 (◆), 65/35 (●) 50/50 (△). (b) Half-time to crystallisation, $t_{1/2}$ for blends of SPS/PPE44 with varying SPS molecular weight, SPS162 (△), SPS292 (◆) and SPS400 (●), at the blend ratios indicated on the figure. (c) Half-time to crystallisation, $t_{1/2}$ for blends of SPS 292/PPE with varying PPE molecular weight, pure SPS (■), 75/25 PPE37 (●), 75/25 PPE44 (◆), 75/25 PPE70 (△), 50/50 PPE40 (★), 50/50 PPE37 (×). The arrow indicates the approximate location of the 50/50 PPE70 series.

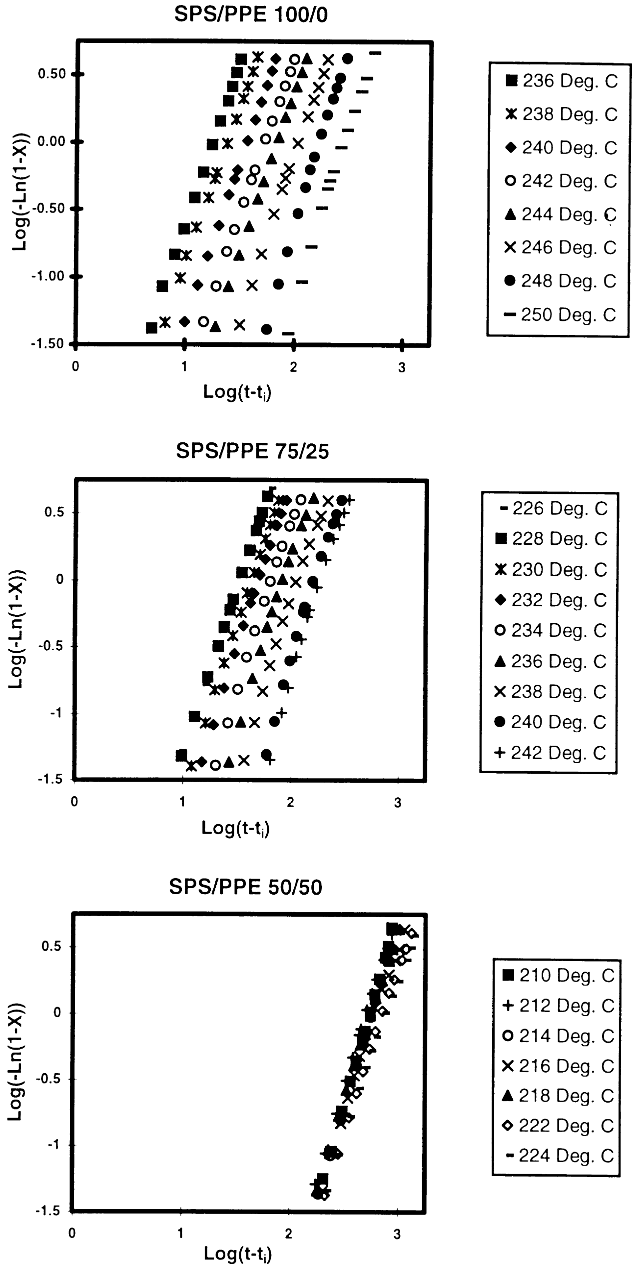

Fig. 4. Avrami plots for the SPS 292/PPE 44 blends.

simulated curves used to calculate the crystallisation parameters through Eq. (12) for the various SPS292/PPE44 blends. Table 3 gives the parameters used for these simulated curves. The starting values for determining the appropriate parameters were those which had been used in work, so far unpublished, on the crystallisation of isotactic polystyrene and these were adjusted iteratively until a fit was obtained. These parameters may not represent unique solutions to Eq. (12), but they do offer data which is useful to the interpretation of the crystallisation process. Table 4 gives the parameters for SPS/PPE blends with varying SPS molecular weight and Table 5 gives the parameters for blends with varying PPE molecular weight. The values of G_0 and U

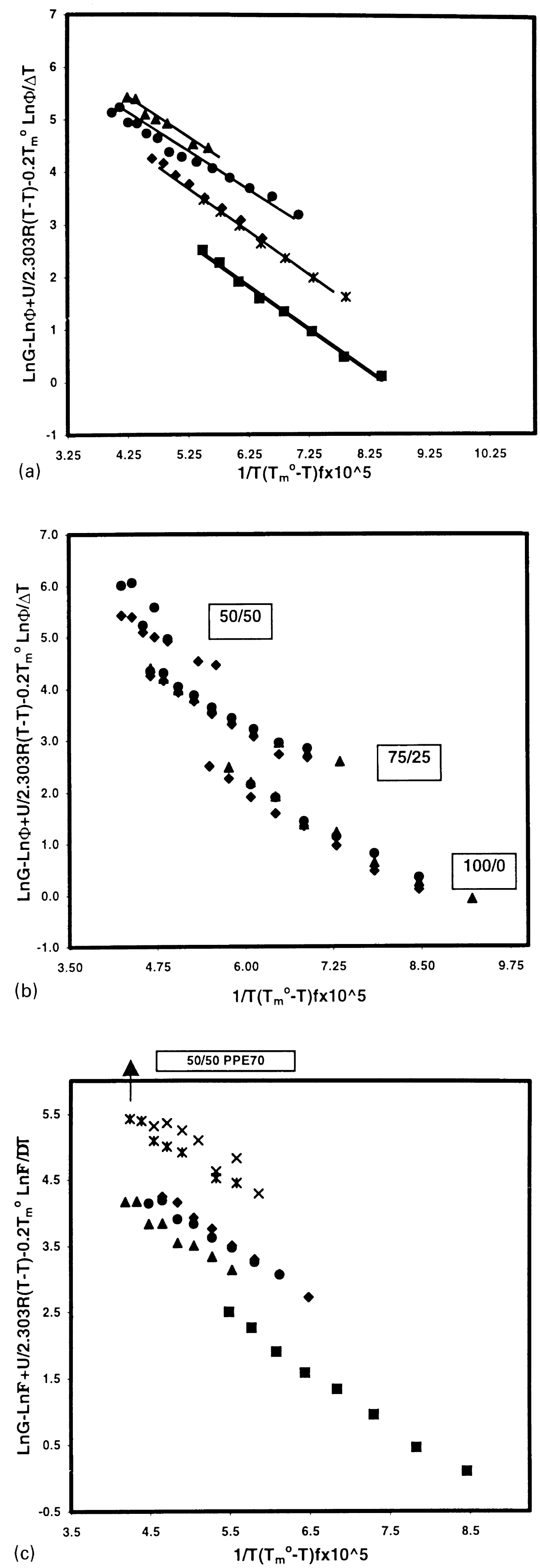

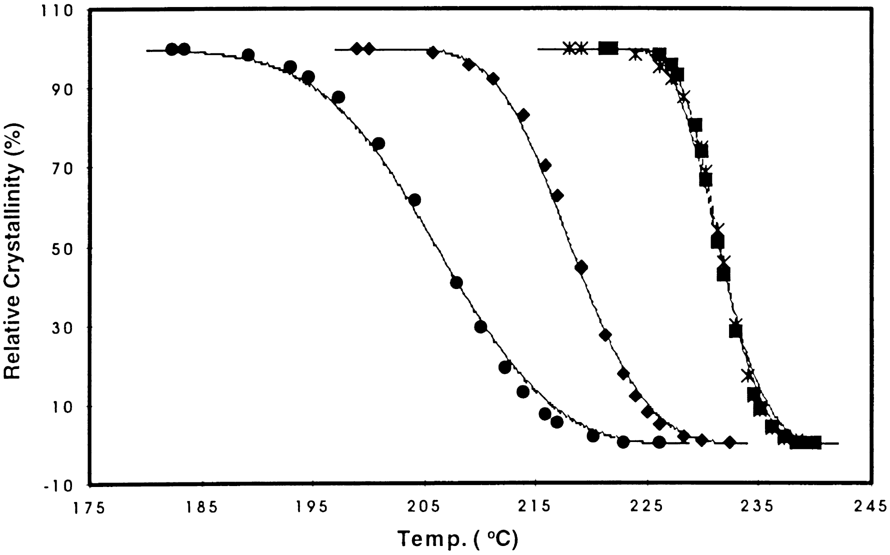

Fig. 6. Relative crystallinity against temperature plot for non-isothermal crystallisation for the SPS292/PPE44 blends, with the simulated curves, shown as a line, used to calculate the crystallisation parameters through use of Eq. (12). SPS, 100 (■), SPS/PPE, 85/25 (★), 75:25 (◆) and 65/35 (●).

can be held constant as the SPS weight fraction is varied suggesting that the SPS weight fraction present does not affect the diffusion process. For the SPS/PPE blend there is a small increase in the thermodynamic constant, *A*, at lower SPS content. This indicates that there is an increase in the thermodynamic force for crystallisation at higher SPS fractions. The diffusion constant, *U* does not increase with molecular weight as might have been expected. The small difference in the values of *U* for the 100/0 material is probably due to experimental error, rather than molecular weight effects. The same can be said for the 75/25 blend. For the 100/0 blends $n = 2.75$ and 2.55 for the 75/25 blends and if this slight difference is significant it may reflect changes in dimensionality or different contributions of homogeneous and heterogeneous nucleation.

The values of *n* are not affected by molecular weight, only by blend ratio and similarly the value of *A*, the thermodynamic coefficient is affected by blend ratio only. However *U*, the diffusion constant does change. It has been assumed that the crystallisation mechanism of the PPE37 and PPE44 series are almost identical with any differences attributed to experimental error. It seems probable that the same assumption can be used here to explain the difference in the values of *U*, 1500 and 1700 cal mol^{-1} for the PPE37 and PPE44 series, respectively. This assumption can be justified by noting the temperatures at which 50% relative crystallinity is reached in the recrystallisation experiments. The temperatures for the PPE37 and PPE44 blends are very close, 218 and 215°C, respectively. The crystallisation of the PPE70 blend is slower with 50% relative crystallinity only reached at 208°C. The crystallisation mechanism of the two lower molecular weight blends are almost identical while the crystallisation mechanism of the third blend is altered by the increased PPE molecular weight. At least one factor in the change of the crystallisation process presumably relates to diffusion problems as the molecular weight of PPE is increased. It is possible that a threshold PPE molecular weight exists below which chain length is not a limiting factor in the diffusion process. However, above this threshold value, the increased length of the PPE chain would lead to greater entanglement, hindering the overall diffusion process. This problem would be exacerbated by the fact that PPE, as the amorphous component, must diffuse away from the crystal growth front in order for crystallisation to continue at an acceptable rate. The threshold value would occur somewhere between an M_w of 43 800 and 70 000.

3.2. Crystal structure

There are four main polymorphs of SPS; (α, β, γ and δ), along with four additional modifications characterised by slightly disordered (α' and β') and highly ordered (α'' and β'') backbones [8]. Given the preparation conditions used in this work it was expected that samples would contain either α or β forms or a mixture of both, but not γ and δ forms [1]. Typical reflection peaks for the α and β polymorphs are given in Table 6.

The diffraction patterns for the SPS292/PPE44

Fig. 5. (a) Lauritzen–Hofmann plots for SPS292/PPE44 blends, SPS, 100 (■), SPS/PPE, 85/25 (★), 75/25 (◆), 65/35 (●) and 50/50 (△). (b) Lauritzen–Hofmann plots for blends of SPS/PPE44 with varying SPS molecular weight, SPS162 (△), SPS292 (◆) and SPS400 (●), at the blend ratios indicated on the figure. (c) Lauritzen–Hofmann plots for SPS292/PPE with varying PPE molecular weight, pure SPS (■), 75/25 PPE37 (●), 75/25 PPE44 (◆), 75/25 PPE70 (△), 50/50 PPE40 (★) and 50/50 PPE37 (×). The arrow indicates the approximate location of the 50/50 PPE70 series.

Table 3
Estimated crystallisation parameters for SPS292/PPE44 measured under non-isothermal conditions

SPS/PPE	100/0	85/15	75/25	65/35
G_0 (cm s^{-1})	26	26	26	26
U (cal mol^{-1})	1500	1500	1500	1500
A (K^2)	300 000	300 000	332 000	355 000
n	2.75	2.75	2.55	2.45

blend series are illustrated in Fig. 7. The four materials; SPS/PPE, 100/0, 85/15, 75/25, and 65/35 have the same overall pattern with only the diffuse scattering increasing as the PPE content increases. There are no α peaks evident (specifically, no peak at $2\theta = 6.7°$). Peaks do however exist at the approximate locations that would indicate the presence of the β polymorph; $2\theta = 6.3$, 12.5, 18.7, and 21.5°.

The β″ polymorph diffraction pattern generally displays a broad peak at an approximate 2θ value of 15.7° [8,22,23]. This peak is not evident in the sample range from SPS/PPE, 100/0 to 65/35, indicating that the polymorph present in these samples is either the β or β′ form. It is not possible to identify the structure any further using only XRD results as there are no discernible differences between the patterns for the β and β′ forms [8,22]. With the SPS/PPE, 50/50 sample, peaks appear at the same approximate locations as for the four materials, 100/0 to 65/35, and in addition, a small peak appears at $2\theta = 6.9°$, with the previous doublet with peaks at $2\theta = 20.2$ and 21.5°, now blended to a single peak at $2\theta = 20.2°$. The peak at $2\theta = 6.9°$ suggests that there is some of the α form present.

Altering the molecular weight of the SPS or the PPE does not have a significant effect on the XRD peak positions, but as shown in Fig. 8, a crystallisation hindering effect is apparent. With the SPS292/PPE70, 50/50 blend the large amount of diffuse scattering almost obscures the peaks.

Table 6
Reflections typical of the α and β polymorphs [8]

Polymorphy	2θ (°)				
α form	6.7	11.7	14.0	15.6	18.0
β form	6.1	12.3	18.6	21.2	

4. Conclusions

The crystallisation of SPS proceeds by heterogeneous nucleation followed by three-dimensional crystal growth, and the crystallisation kinetics are consistent with a regime II process as defined by the Lauritzen–Hoffman approach. The crystallisation rate is affected by blending with PPE with the melting enthalpy of the SPS decreasing and the half-time to crystallisation increasing with PPE concentration. The crystal structure in the materials examined is thought to be of the β or β′ form.

Altering the SPS molecular weight has a negligible effect on crystallisation. This contrasts with the conclusions of Wesson who examined the crystallisation of SPS and found that the molecular weight does affect the rate of crystallisation with lower molecular weight samples crystallising faster at lower temperatures and higher molecular weight samples having the fastest crystallisation rate at higher temperatures [5]. The difference in observation is not thought to be associated with the range of molecular weight used in the two separate studies ($M_w =$ 162 000–400 000 here and 348 000–803 000 for Wesson), rather it arises from the temperatures at which crystallisation was examined (close to T_m here, and T_g to T_m for Wesson). Wesson states that at higher T_c, it is the thermodynamics of crystallisation that provide the rate limiting step, and not the diffusion process. As this study examined only higher T_c it is thus to be expected that altering the SPS molecular weight would not affect the crystallisation

Table 4
Estimated crystallisation parameters for SPS/PPE blends with varying SPS molecular weight measured under non-isothermal conditions

Material parameters	SPS162 (100/0)	SPS292 (100/0)	SPS400 (100/0)	SPS162 (75/25)	SPS292 (75/25)	SPS400 (75/25)
G_0 (cm s^{-1})	26	26	26	26	26	26
U (cal mol^{-1})	1300	1500	1300	1410	1500	1300
A (K^2)	300 000	300 000	300 000	332 000	332 000	332 000
n	2.75	2.75	2.75	2.55	2.55	2.55

Table 5
Estimated crystallisation parameters for SPS/PPE blends with varying PPE molecular weight measured under non-isothermal conditions

Material parameters	SPS292 (100/0)	PPE37 (75/25)	PPE44 (75/25)	PPE70 (75/25)
G_0 (cm s^{-1})	26	26	26	26
U (cal mol^{-1})	1500	1700	1500	1940
A (K^2)	300 000	332 000	332 000	332 000
n	2.75	2.55	2.55	2.55

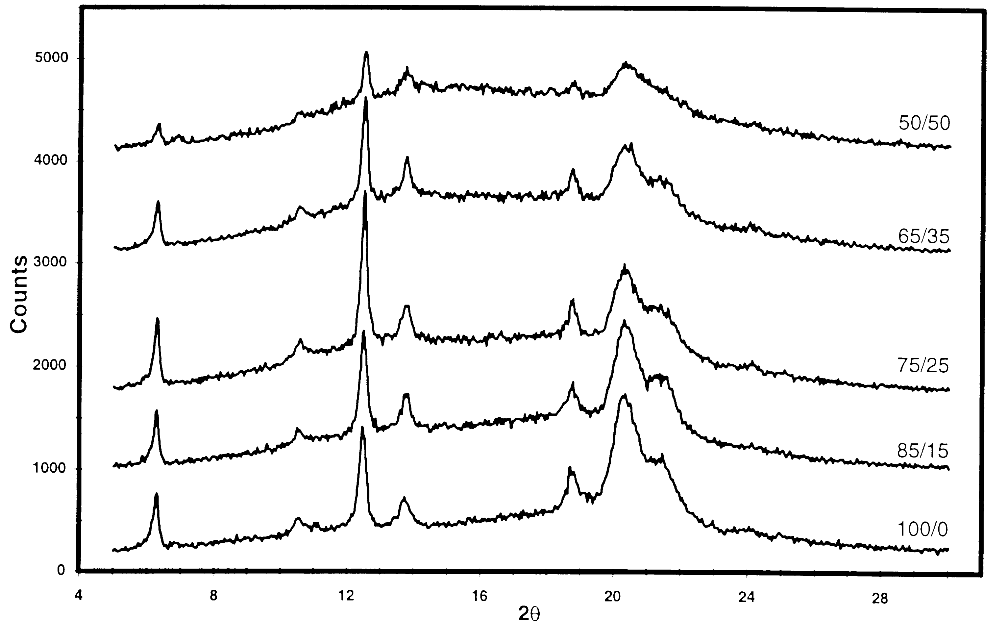

Fig. 7. X-ray diffraction patterns of SPS292/PPE44 blend series.

process greatly, particularly as the range of SPS molecular weight examined here was relatively small. It is more to be expected that altering the SPS molecular weight would have much greater effect at lower temperatures, close to T_g. The SPS molecular weight in this work was limited by the synthesis method available and so a direct comparison between the two studies is not possible.

The crystallisation of SPS is affected by the molecular weight of PPE. The half-times to crystallisation and the Lauritzen–Hoffman plots both indicate that varying the PPE molecular weight affects crystallisation, but this is most evident in the XRD patterns which show clear interference from the higher chain length PPE. Crystallisation in a polymer blend involves two types of polymer transport; diffusion of the crystallisable component towards the crystal growth front and a simultaneous rejection of the amorphous components. The non-isothermal data indicates that the diffusion constant changes with PPE molecular weight. It appears that the overall lack of flexibility of PPE (indicated by its relatively high T_g compared to that of SPS) combined

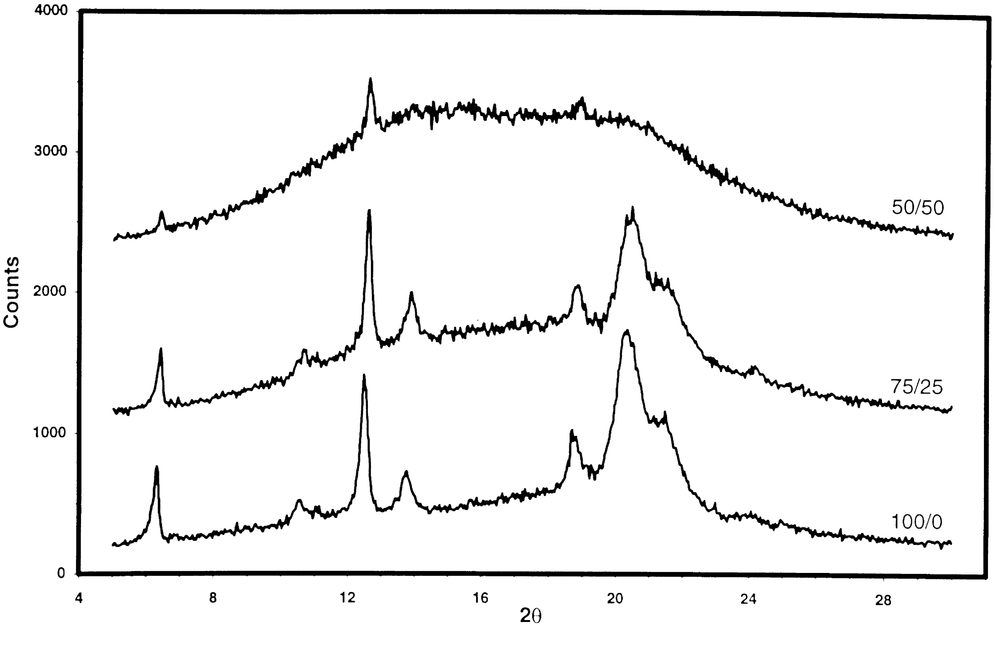

Fig. 8. X-ray diffraction patterns of SPS292/PPE70 blend series.

with increased length at higher molecular weights leads to an increased number of chain entanglements and diffusion difficulties. Given that PPE is the amorphous component of the blend and must diffuse away from the crystal growth front in order for crystallisation to continue at an acceptable rate it is thus reasonable that PPE will have a major effect on SPS crystallisation, particularly at higher concentrations.

References

[1] Kellar EJC, Galiotis C, Andrews EH. Macromolecules 1996;29:3515.
[2] Brinklow D. Polym News 1996;21:316.
[3] Park JY, Park OO. Jpn J Rheol 1997;25:25.
[4] Cimmino S, Di Pace E, Martuscelli E, Silvestre C. Polymer 1991;32:1080.
[5] Wesson RD. Polym Engng Sci 1994;34:1157.
[6] Stlawrence S, Shinozaki DM. Polym Engng Sci 1997;37:1825.
[7] Cimmino S, Di Pace E, Silvestre C. Polymer 1993;34:2799.
[8] Guerra G, De Rosa C, Vitagliano V, Petraccone V, Corradini PJ. J Polym Sci Part B: Polym Phys Ed 1991;29:265.
[9] Avrami M. J Chem Phys 1939;7:1103.
[10] Avrami M. J Chem Phys 1940;8:212.
[11] Hoffman JD, Davis GT, Lauritzen JI. The rate of crystallisation of linear polymers with chain folding. In: Hannay NB, editor. Treatise on solid state chemistry. New York: Plenum Press, 1976. p. 497–614.
[12] Wang YF, Lloyd DR. Polymer 1993;34:4740.
[13] Lim GBA, Lloyd DR. Polym Engng Sci 1993;33:513.
[14] Lim GBA, Lloyd DR. Polym Engng Sci 1993;33:522.
[15] Martuscelli E, Riva F, Sellitti C, Silvestre C. Polymer 1985;26:270.
[16] Bartczak A, Galeski A, Pracella M. Polymer 1986;27:537–43.
[17] Ong CJ, Price FP. J Polym Sci Polym Symp 1978;63:59.
[18] Wunderlich B. Macromolecular physics, vol. 2. New York: Academic Press, 1976.
[19] Hoffman JD, Weeks JJ. J Res Natl Bur Stand 1962;66A:13.
[20] Nakamura K, Katayama K, Amano T. J Appl Polym Sci 1973;17:1031.
[21] Agin G. SIMULSOLV Computer Program, Dow Central Research Department, 1986.
[22] Guerra G, De Rosa C, Vitagliano V, Petraccone V, Corradini P. Macromolecules 1990;23:1539.
[23] Guerra G, De Rosa C, Vitagliano V, Petraccone V, Corradini P, Karasz FE. Polym Commun 1991;32:30.